EPJB manuscript No.
(will be inserted by the editor)

A 1D ion chain on a laser field: a Wigner solid with vacancies

W. Quapp[1] and J. M. Bofill[2]

[1] Mathematisches Institut, Universität Leipzig, PF 100920, D-04009 Leipzig, Germany
(ORCID: 0000-0002-0366-1408) e-mail: quapp@math.uni-leipzig.de
[2] Departament de Química Inorgànica i Orgànica, Secció de Química Orgànica, and Institut de Química Teòrica i Computacional, (IQTCUB), Universitat de Barcelona, Martí i Franquès 1, 08028 Barcelona, Spain
(ORCID: 0000-0002-0974-4618) e-mail: jmbofill@ub.edu

Received: June 27, 2025/ Revised: August 25, 2025/ Accepted:

Abstract. Trapped ions in a periodic potential are a paradigm of a frustrated Wigner crystal. We study a model for a 1D chain of such ions, as well as an approximation by a Frenkel-Kontorova model. The FK model, however, has other long-range properties. We discuss the meaning of structures like kink or antikink in the frame of the soliton theory, and that ion chains with large distances against the laser frame can have difficulties to move solitons. We study the case with 3 particles only for which all important properties can be demonstrated.

Key words. 1D ion systems – Winger solid – Frenkel-Kontorova model – Newton trajectory – Kink/antikink motion

PACS. XX.XX.XX No PACS code given

1 Introduction

A Wigner solid (WS) is an experimental fact [1–3] that has first been observed in a system of two-dimensional surface-state electrons floating above a liquid helium-4 surface [4, 5]. Trapped ions in a periodic potential are another paradigm of a frustrated Wigner crystal. Here we discuss the substitution of a Coulomb potential of a WS chain by harmonic potentials in a Frenkel-Kontorova chain (FK) [6, 7].

The focus of research of WS properties concerns electron chains in one- or two dimensional structures [8–17], which are often investigated using Luttinger-liquid theory [18,19]. In contrast, the ionic chain which we treat is formed by bosons. The WS gives rise to many interesting phenomena, such as the stick-slip motion of a WS [20–22], and the finite-size effect of WSs on sliding transition [23,24]. Ion chains can be used for quantum simulations and quantum computing [25–31]. A special form of a WS are chains of electrons in a carbon tube [32–37]. The competition between the collective behavior of the correlated particles and the influence of the environment on individual particles is important for many-particle problems [38]. The connection to the Hubbard model [39,40] is interesting. Chains of laser-cooled ions in linear Paul traps are paradigmatic realizations of a harmonic crystal in one dimension [41,42]. The nonlinear transport properties observed in the aforementioned works essentially result from the coupling of WSs and a laser field. In these systems, order emerges from the interplay between the Coulomb repulsion and the trapping potential. Even in one dimension, the long-range nature of Coulomb interactions warrants diagonal (quasi) long-range order, and any finite chain is effectively a one-dimensional Wigner crystal [2]. Transverse degrees of freedom are of interest and they are decoupled from longitudinal degrees of freedom [34]. At the typical temperatures reached by laser cooling the ions vibrate harmonically at the crystal equilibrium position and their motion is described by an elastic crystal with power-law coupling [43]. The ion chain is simply equilibrated at the minima of the potential, however with electron chains we have the more complicated problems of long-range pairing or long-range hopping [44]. The experimental capability to image and monitor the individual ions makes ion chains a prominent platform for studying structural phase transitions [45–48] and the static and dynamic properties of crystal dislocations [49–56]. The progress in cooling and trapping [57] paves the way for investigating these dynamics deep in the quantum regime [58–63].

We understand the WS as a chain of particles and report here on a numerical study of a 1D model WS. The Coulomb potential between ions is not screened by the presence of other ions. We understand a laser field like an additional substrate potential. This periodic substrate potential is assumed to be a sinusoidal function. The two outer ions are assumed to sit near minima of the substrate. The chain is really of finite length. In the ground state, the boundary condition is then a nearly zero amplitude of

the two outer ions. We search the form of the movement of a 1D WS through a substrate potential. Here are assumed large voids between the ions. We will see that such vacancies destroy the possibility of solitons.

On the other hand, fixed boundary conditions for the particles x_1 and x_N of the chain [7] would destroy a model of a finite, but freely moving chain [64]. So we leave free the boundary conditions of the chain, and it can move like in the experiment under an external excitation, for example by a laser field [23,24,65,66].

Newton trajectories (NT) describe the moving stationary points of the potential energy surface (PES) under an external force. The NTs are curves in the configuration space of the chain. The NT theory was discussed in Refs. [67–70] to name a few. They are curves where at every point the gradient of the PES points into the same direction, called the search direction. If we compress or pull the chain, some or all coordinates of the ions change. Some examples of a changed chain are drawn below. Every point of an NT is a configuration of the chain. We treat the PES here like in chemistry where reaction paths describe movements of the molecule over saddles (SP) of the PES [71,72]. To a given driving force, the search direction, on any number of chain ions, we get the 'static' curve of the NT on the PES of the movement of the stationary points of the chain. For practical reasons, we divide an NT into M nodes. The number of nodes used depends on the step length of the predictor of the NT program.

We find that the chain not moves as an inelastic, 'solid' body, or with a 'collective sliding', if the trapping laser field has a certain strongness. The black spaces between the ions in this model are the reason, schematically shown in Fig. 1. The chain of ions in the drain of an experiment will be picked up by an external force (see Eq.(3) below).

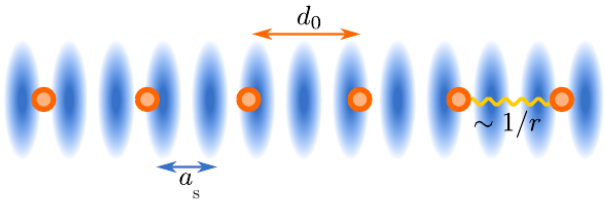

Fig. 1. Illustration of a trapped-ion model. N=6 cold ions (dots) at assumed average distance d_0 under the Coulomb repulsion. The ions are interacting with the standing wave of a laser field (shades), forming a periodic potential with periodicity a_s. We assume $d_0 \gg a_s$ causing barenesses between the ions. Courtesy Ref.[7].

A kink is a stretched structure of a part of the chain where an antikink is its compressed counterpart. In an abstract imagination, for many parameters of the chain [22,73–75], these are 'quasi particles' which can move like a wave through the chain along a flat valley of the N-dimensional PES. However for a chain of ions with larger distances than the laser ground field, compare Fig.1, such structures are questionable, see our study below. We understand kinks and anti-kinks as descriptions of solitons [76], but not as simple distortions of the chain [77]. A soliton is a nonlinear, self-reinforcing, localized wave packet that is stable [76]. It preserves its shape while propagating more or less freely, at constant velocity, through the chain. The remarkable stability of a soliton in a dense FK chain can be traced to a balanced action of two potentials. To achieve the soliton behavior, we study the PES of the chain and search for a pathway in the mountains, however, which is there quite flat. The soliton wave can move there after a push over the so called Peierls-Nabarro barrier [78].

This paper is a new part to a series of works to the Frenkel-Kontorova model [22,75,79–86]. In our previous work [79] we found kinks in commensurate and in incommensurate lattices. Here in this case with large distances between the ions, we do not find sliding antikinks, kinks or pairs of them doing the movement of the chain. It is in contrast to Refs. [7,56] where the authors claim that kinks are possible and are an indicator for incommensurate lattices.

We report: The ground state is in any case a global minimum of the PES. If there exist a substrate potential then there exist global minima, and we cannot see any kind of a fractal ground state of the ion chain [7]. If no external force acts then no stip-slick motion can take place. Thus a general sliding-to-pinned transitions [7] is to reject. We show that the imagination of a soliton like movement of an ionic chain with large gaps in relation to the trap potential is not correct. The claim of a kink structure of a WS [7], especially, is to reject.

In section 2 we introduce the WS model used in this paper. Section 3 enrols the FK approximation of the WS for N=3 and studies the impossibility of kinks and antikinks. Section 4 comes back to the WS model itself. We find a partial soliton like property for a special region of the parameters of the chain, indeed, though we assume a vacancy. A Discussion and Conclusions are finally given.

2 A model for a Wigner solid

$\mathbf{x}^T = (x_1, ..., x_N)$ represents the position of N discrete particles of a chain, here ions of the Wigner crystal. Bold letters depict vectors. The positions x_i are on a linear axis. It holds $x_i < x_{i+1}$. We treat a finite chain. The free end points of the chain determine the average distance $d_o = (x_N - x_1)/(N-1)$. It is determined by the density of the ions. Caused by the experiment, we have an integer number of ions in an integer number of trapping bowls, so there is always given a rational relation. Between the repelling ions we have the long-range Coulomb potential [7,48,87]

$$V_W(\mathbf{x}) = \frac{W_o}{2} \sum_{j=2}^{N} \sum_{1=1}^{j-1} \frac{1}{|x_j - x_i|^\alpha} + \sum_{i=1}^{N} V_s(x_i), \qquad (1)$$

where charge W_o=2 is a parameter, and α=2 is specified here. (For this α we can avoid the amount bars || in the repulsions.) All parameters are used in dimensionless form.

The substrate potential is

$$V_s(x) = \frac{V_o}{2}\,(1 - cos(\frac{2\,\pi}{0.6}\,x))$$

with periodicity $a_s = 0.6$ and V_o=1/2. This V_o is in the interval $(0.03, 1.066)$ of Ref. [7]. The function V_s forms the axial confinement. If $V_o > 0$ then a finite chain will always be locked [88]. We treat N=3 ions for 6 wells of the laser, so, the half of the extension of Fig. 1. (The case N=2 for electrons is being studied intensively [17,35,89]. The somewhat simpler ions enable the next case N=3 here.) The distance $d_o = 1.5$. Note that we do not have a dependence on this d_o distance in the Coulomb ansatz; this distance is determined by the density of the ions in the experiment. The periodicity a_s is still large enough to assume that the ions interact like point charges [4].

A PES section for fixed x_1 and x_3 (red dots) is shown in Fig. 2. There exist two minima where both of which can form a chain structure. If we leave free the boundary ions x_1 and x_3 we get the two minima of the chains at (-0.04, 1.22, 3.016) or (-0.015, 1.78, 3.04) length units. Thus the ions are spaced non-uniform. This will be of importance for the question of the existence of solitons below.

The chain has the following eigen system: The three eigenvalues for the left version with x_2=1.22 are λ_1=31.11, λ_2=27.73, λ_3=25.85 with the corresponding eigenvectors e_1={0.54, -0.83, 0.13}, e_2={-0.24, 0, 0.97}, and e_3={-0.81, -0.55, -0.2}. e_1 and e_3 are mainly the quasi-symmetric and antisymmetric vibrations between x_1 and x_2 while e_2 is the quasi-symmetric vibration between x_1 and x_3.

Note that the representation in Fig. 2 with fixed edge ions x_1 and x_3 covers up the problem that the Wigner chain with potential (1) has no stable end ions by itself. If not fixed by the substrate potential, they move away and the chain destroyes itself. Without the part $V_s(x)$ the chain would spread to the left and to the right hand side without a border. This also means that the amplitude of V_s must have a certain amount.

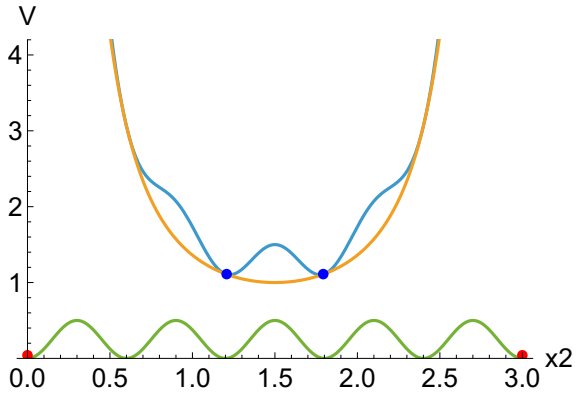

Fig. 2. The energy profile of ion x_2 in blue for $\alpha = 2$ in Eq.(1). It is the sum of the green and the dark yellow curves. a_s=0.6, and the length of the chain is L=3. Green is the substrate potential, but dark yellow is the repulsion of the central ion x_2 by x_1 and x_3 (red dots). There are two equivalent minima for x_2: blue bullets. Note that the ion x_2 is artificially lifted on the potential line. The real chain is on a straight line. Only the distances can change.

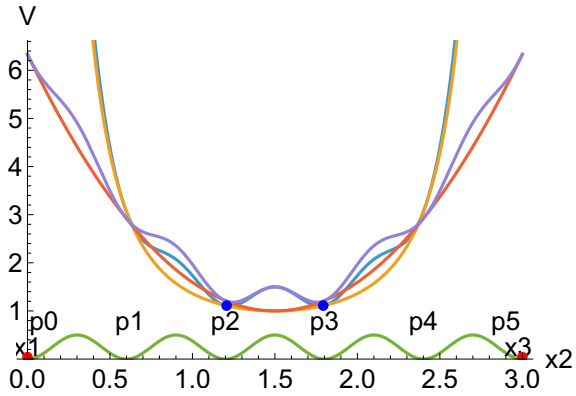

Fig. 3. Additional included is the red curve: the approach (2). It is qualitatively similar to Fig. 2 near the minima. The p i are positions on the substrate potential: p0 is position of the here fixed x_1=0, p2 and p3 are possible positions of x_2, but p5 is x_3=3 also fixed. Positions p1 and p4 are bareness.

3 An approach to replace the Wigner solid by a Frenkel-Kontorova model

The study of the Wigner chain will be postponed until Section 4. One can change the treated PES to a quadratic Frenkel-Kontorova form [7] not only with nearest neighbor terms but also with further long-range interactions [90,91]. The new PES is again combined from two parts, compare Fig.3. It is [6,7]

$$V(x_1,x_2,x_3) = \sum_{i=1}^{3} V_s(x_i) + \frac{k}{2}\,((x_3 - x_2 - d_o)^2 + (x_2 - x_1 - d_o)^2 + \frac{1}{2^4}(x_3 - x_1 - 2d_o)^2)\ . (2)$$

The factor k is defined by the former potential through

$$k = \frac{\alpha(\alpha+1)\,W_o}{d_o^{\alpha+2}}$$

so here by $k = 2.37$. This FK model is not the Taylor approximation of potential (1) like it is claimed in Ref. [7]. It is simply a nice polynomial approximation [12]. There is a next-nearest neighbor term, thus we have a modified Hamiltonian [92] against the original FK model. The change of the model equation is locally quite appropriate in comparison to Eq.(1), however, it does now also fit the outer two ions. The minima states of both potentials are nearly equal, and one can calculate small local vibrations [43,93,94]. However, if the single ions come nearer together then the potentials (1) and (2) are different. The Coulomb potential (1) has singularities, but the FK potential (2) not. It is to observe in Fig. 4 where no singularity emerges.

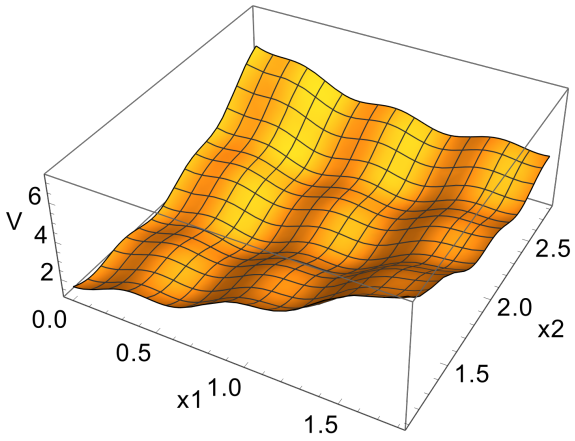

Fig. 4. PES section of the FK model over x_1 and x_2, but $x_3 = 3$ is fixed.

3.1 Search for anti-kinks

The aim of this subsection is a numerical study concerning the possible existence of solitons. First, the outer ions x_1 and x_3 are put in the outer bowls of the substrate potential at $x_1 \approx 0$ and $x_3 \approx 3$. There are 6 bowls in sum. Then ion x_2 could be in 4 different bowls in between, and there are indeed 2 different minima of the PES (2), at positions p2 and p3, compare the 2D-section of Fig.4 also. Because the middle value x_2 at 1.5 is a saddle point (SP) of the PES, the two global minima are asymmetric to x_1 and x_3, see Figs.2 to 4. There are $L/a_s = 5$ peaks of the laser field in between. Without the border ions x_1 and x_N there are for the N-ionic chain $N-2$ internal ions for $N_s - 2$ bowls. The equations for the calculation of the stationary points are usual nonlinear coupled equations which are solvable without a Fourier transformation [7]. Note that one should not use periodic boundary conditions (BC) [7] for a linear chain, which one needs for the Fourier transformation only. If one will study a moving chain caused by pulls or pushes (a soliton like case) then fixed BC are excluded. Of course for rings of ions hold periodic BC [95].

One should also observe that the outer parts of the potentials (1) and (2) are qualitatively different. For a large enough force in the FK model, an x_j can move over an x_{j+1}. This should be forbidden by the definition of the chain. It is a gap of the model (2).

Fig. 5 shows the potential profiles of a free ion x_2 under fixed x_1 and x_3 positions. Where x_3 is fixed at 3 throughout, but x_1 moves over the substrate potential. x_1=$\{0, 0.6, 1.2\}$ are minima and stationary x_2-curve points show the correct index. x_1=$\{0.3, 0.9\}$ are SPs of x_1, thus the corresponding minima of the x_2-curves are transition states (TSs) of index one, but SPs of the x_2-curves are TSs of index two. Fig. 6 shows in contrast the profile of a moving x_1 for fixed values of x_2 and x_3.

A movement of a chain [20,66] may be forced by an external excitation with a linear unit force $\mathbf{f}$ of amount F by the effective potential

$$V_{eff}(\mathbf{x}) = V(\mathbf{x}) - F\,\mathbf{f}^T\,\mathbf{x}\ . \qquad (3)$$

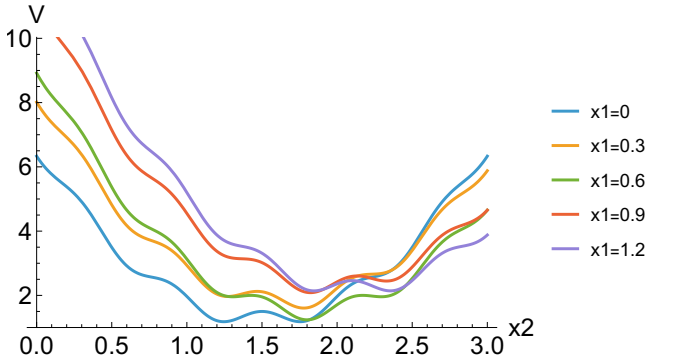

Fig. 5. Potential curves for x_2 under different fixed values of x_1 and fixed $x_3 = 3$, see text.

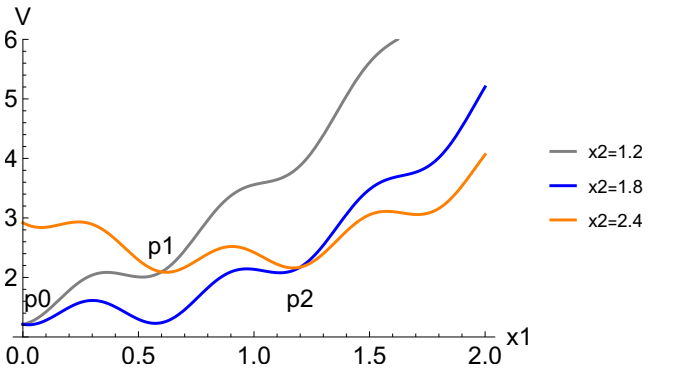

Fig. 6. Potential curves for x_1 by different fixed values of x_2 at p2 or p3 and fixed x_3=3. The potential sections are orthogonal to the former Fig. 5.

F zero is the original PES, but for an increasing force the stationary points of V_{eff} move. The calculation of this pathway is given by Newton trajectories (NT) [64, 96]. NTs have the nice property that they connect stationary points of the original PES. If no turning point (TP) emerges, they can be used as a model for the minimum energy path (MEP) between SP and minimum. We imagine a chain ground state at $\mathbf{x}^T$= (0, 1.2, 3). A force acting only on x_1, thus in direction $\mathbf{f}^T$=(1, 0, 0), can move the ion x_1 to position p1, compare the gray curve in Fig. 6. In Fig. 7 it is at the position at the right minimum at (0.53, 1.29). The blue curve in Fig. 7 is the NT to the given direction on the PES with fixed x_3=3. The blue dots are from a calculated NT on the full 3D PES with free x_3. Both curves are near identical. Thus the 2D projection of Fig. 7 is a good approximation of the full dimensional problem. Note that NTs describe the movement of stationary points under the force $F\,\mathbf{f}^T$ on the effective PES $V_{eff}(\mathbf{x})$. The green lines are the index boundaries (IB) of the Hessian matrix given by $Det(\mathbf{H}) = 0$. They are drawn for orientation on the PES. Closed green regions describe the regions of minima with index zero of the Hessian, regions of an SP with index one, or of a maximum with index two.

Further pressure into the same direction would move the outer ion to position p2, however there is no further minimum of the PES. Already the ion x_2 is sitting there. The amount of force may be larger, however, the ion x_2

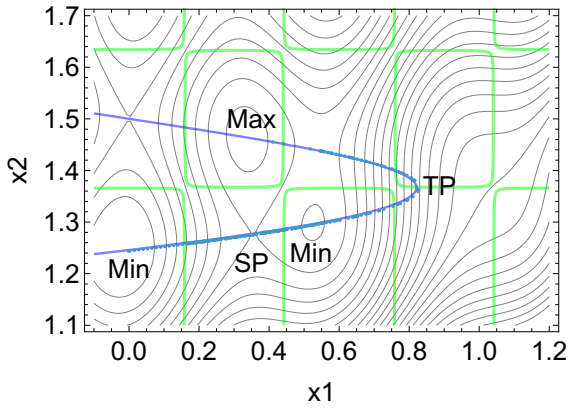

Fig. 7. 2D PES section for x_1 and x_2 and fixed x_3=3. The blue dotted curve is the NT to direction $(1, 0, 0)$. It has a turning point TP, but does not find the direction to the next x_2 minimum at $(0.6, 1.8)$ units.

must not evade. It is not really pushed away on the assumed PES (2), in contrast, for example, to a chain in ref [22]. A corresponding NT ends at a turning point (TP) in the PES 'mountains'. The valley after minimum p1 for x_1 is a 'dead' valley. The PES (2) causes too less repulsion between the ions.

If the compressed structure would behave like an anti-kink then the ion x_1 had to push the ion x_2 away under its own pressure. However this does not happen. The valley from structure $\mathbf{x}^T \approx (0.6, 1.2, 3)$ to $\mathbf{x}^T \approx (0.6, 1.8, 3)$ is relatively flat, but there is no force to push the first to the second state.

If the ion x_2 has found a way to jump to position p3, for example by its zero point vibration, then an analogous situation like in Fig. 7 emerges, shown in Fig. 8. The force $(1, 0, 0)$ pushes only x_1 along the valley up to high values of energy, however, again there does not open a door for the jump to p4 for ion x_2. Especially, x_3 is not moved.

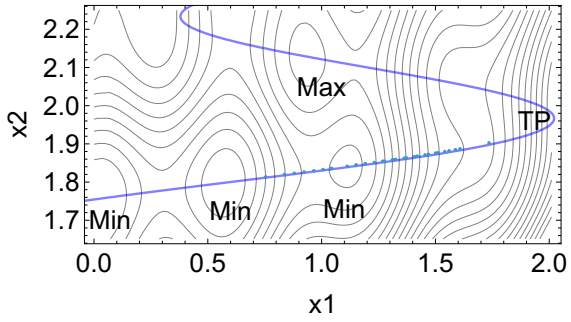

Fig. 8. 2D PES section for x_1 and x_2 and fixed x_3=3 for x_2 near 1.8, thus position p3. The blue curve is the NT to direction $(1, 0, 0)$. It has again a turning point TP far in the mountains, but does not find the direction to the next x_2 minimum at 2.4 units at p4. The three minima correspond to positions p0, p1, and p2 for ion x_1 on the blue profile in Fig. 6.

The central property of such an ion chain with vacancies is that every ion of the chain can relax from an SP on the substrate potential to a next isolated minimum of the laser field without to push stronger the other ions out of their equilibrium positions. It is a fundamental property of this kind of chain caused by its vacancies between the ions, compare Fig. 4 (where there x_3 is still fixed). One must remark that the profile of this movement does not look like a profile for the movement of a soliton [79,80]. It is in contrast to a claim of refs.[7,97] where a soliton like behavior also for ion chains with gaps is assumed.

3.2 A collective excitation

If we push the chain in a collective excitation to direction $\mathbf{f}^T = 1/\sqrt{2}\,(1, 1, 0)$ we can move two ions to two neighboring positions, but this is not the idea of a soliton, compare Figs. 9 and 10. The chain behaves like a harmonica. No single soliton wave of an anti-kink will move along the chain. Note that the magenta NT describes a minimum energy path (MEP) through two quasi orthogonal valleys, though the search direction points diagonal in the Figure. Contrary to the idea of a soliton, the movement first is done by ion x_2, and followed by a move of x_1. This NT can be used for a description of the corresponding movement of the initial part of the chain.

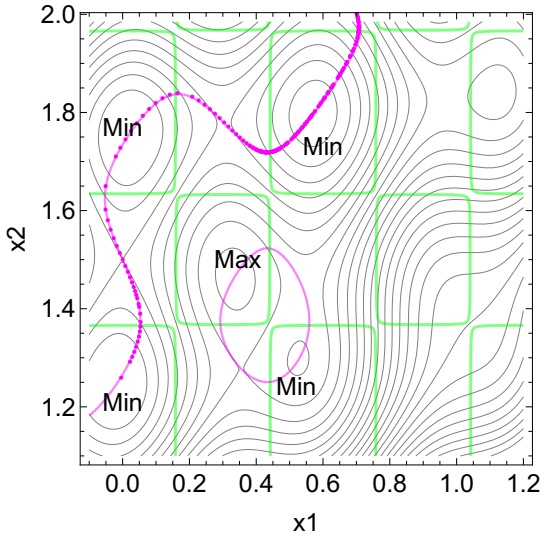

Fig. 9. 2D PES section for x_1 and x_2 and fixed x_3=3. The magenta dotted curve is an NT to direction $(1, 1, 0)$. It reaches the next x_2 minimum at $(0.6, 1.8)$ units by a MEP.

3.3 Search for the minimum energy path (MEP) for a kink

A so called kink can happen after a pull of the right border ion to the right hand side one bowl further. Note that we name 'kink' not only a distortion of the chain [97]. So, if one pulls the last ion x_N out of the chain then may emerge

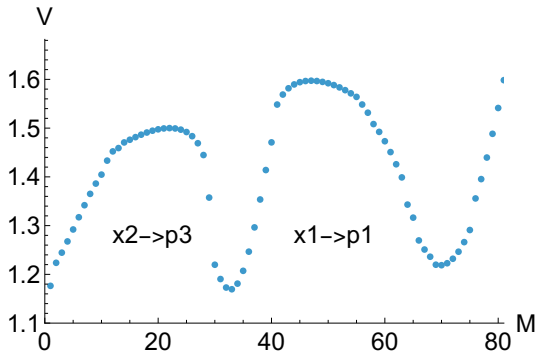

Fig. 10. Potential profile for the MEP of Fig. 9 of a move of parts of the chain by one period of the substrate potential, a move for ions x_2 and x_1: the left peak is the pathway of x_2 to position p3, after that the way of x_1 follows, from p0 to p1 (again a minimum).

a kink, for which the distortion should wander through the chain backwards.

This does not happen here, in analogy to the former test for an anti-kink. In Fig. 11 we show an NT to the pure pulling direction of x_3. The pull may move the x_3 to a next minimum, but later does not equivalently move ion x_2. In contrast the NT again runs up to a TP and comes back to a maximum in between. The chain may jump by its internal zero point vibration to the next, whished minimum at point $(0, 1.8, 3.57)$. However, here again emerges the relation analogous that the pulling goes only along the x_3 valley. So, no kink behaviour is to constate. (One may observe the symmetry to the antikink test of Fig. 7.)

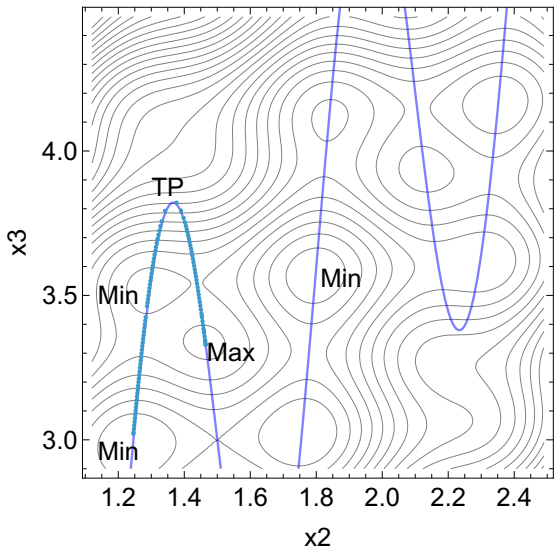

Fig. 11. PES section for x_2 and x_3 under fixed x_1=0. Blue is the NT to direction $(0, 0, 1)$. Blue points are calculated by a 3D NT on the full surface.

We conclude that PES (2) with the given parameters and with vacancies between the ions does not allow kinks or antikinks.

4 The Wigner chain

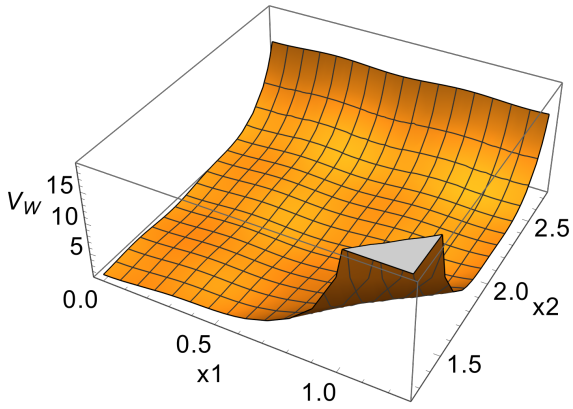

Fig. 12. Case N=3, 2D section of PES (1) for fixed x_3=3, in contrast to Fig. 4.

We still have to compare the potentials (1) and (2). Fig. 12 represents correctly the repulsion between the ions in the chain for potential (1). The PES becomes infinite for a touching of the ions, in contrast to the case of PES (2). It is clear that we cannot hope for a soliton like kink in a Wigner chain, because there are no springs which hold the ions together. Only the bowls of the field do this. If one pulls out the last ion x_N then it leaves the chain without any counter-force. We have to conclude that the idea of a kink for potential (1) is not correct.

In contrast, in the FK model Eq.(2) there may be a 'spring' force which pulls piece by piece of the chain further, if we pull strongly x_N. But we have seen that a wave of such a kink through the chain again does not happen because of the vacancies of the chain.

4.1 Are there anti-kinks in a Wigner chain?

Fig. 13 is the analogous PES projection for fixed x_3=3 like Figs.7 and 8, but now for the Wigner potential (1). The IB lines are again drawn in green, and the blue line is the NT to direction $(1, 0, 0)$. To come from the minimum Min1 left below to the minimum Min3 right above, there is first a MEP for x_2 at the left hand side to the minimum Min2 at $(0, 1.8)$, and then the horizontal path for x_1 to the aim. The figure has a certain similarity to the FK case, however, the repulsion of the ions is stronger, and this makes another relation between the two minima of interest, the original Min1 at $(0, 1.2)$, and this of Min3 at $(0.6, 1.8)$ after a move by one period of the substrate potential. Here a direct SP emerges on a diagonal pathway, and a former intermediate minimum is missing. By red dots are included the points of a SD calculation from the SP, see Figs. 13 and 14.

If one excites the left outer ion x_1 of the ground state p0-p2-p5 of the chain by a force then this SP comes into the play. With this Fig. 13 we can assume that a push of the outer ion x_1 can lead over this SP to a movement of the

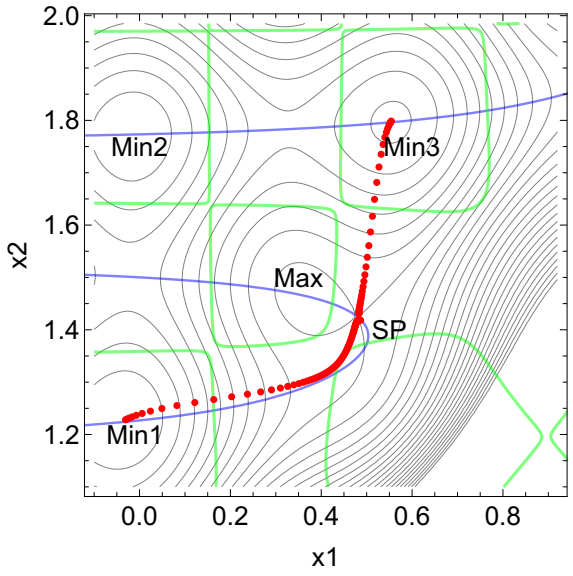

Fig. 13. 2D section of PES (1) for fixed x_3=3, with NT to direction $(1, 0, 0)$. Compare Figs.7 and 8. Red dots form the steepest descent (SD) from the given SP.

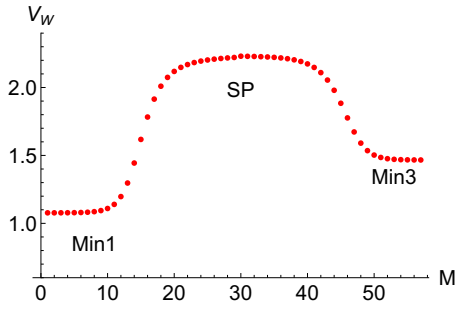

Fig. 14. Energy for a partial soliton like move of two neighboring ions along the SD diagonal path in Fig. 13.

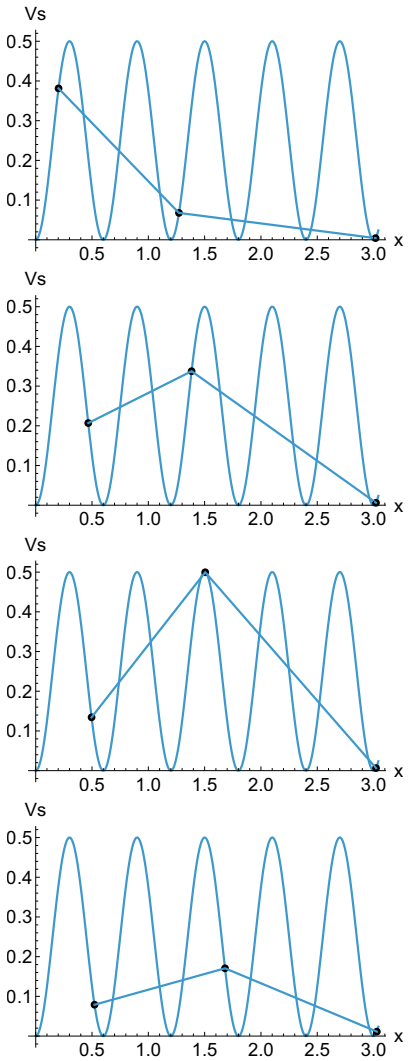

Fig. 15. Snapshots of the chain on the SD pathways of Fig. 13. Only the pair (x_1, x_2) moves in a combined kind, but x_3 is quasi not included. The ions are artificially lifted on the substrate potential line.

couple $(\mathrm{x}_1, \mathrm{x}_2)$ into the minimum Min3 at $(0.6, 1.8)$. This is, so to say, a partial soliton for the couple. The energy step to the SP is 1.1 energy units, see Fig. 14, and the push of ion x_1 leads in a soliton like push to an equivalent move of ion x_2. A series of snapshots of this movement is shown in Fig. 15. Note that two ions have to overcome two barriers of the substrate, but there is on the pathway of the red dots only one SP for this movement.

However, it is again not the pattern of a 'full' soliton because at the end of the push, an intermediate deep minimum exists, Min3. It does not exist the quasi energy less possibility of a further movement of the x_1-distortion to push the next ion x_3 one bowl further, in a here not shown third dimension. It is deeper reported in Fig. 16. It is the effective PES projection for fixed x_3=3 but under the force $\mathbf{f}$=2.25 $(1, 0, 0)^T$. The diagonal SP becomes lower than the left SP for a movement of x_2 alone, for x_1=0. Additionally the calculated NT on the full 3D PES is overlayed by blue dots. The calculation of the NT for this partly singular potential (1) is not fully stable. It jumps after the SP region into the upper valley, onto the upper branch of the NT. But it demonstrates that the 2D projection for fixed x_3 is a good approximation of the full 3D-problem. The upper branch of the blue NT in Fig. 16 leads to a new minimum Min4 for x_1. The reason is that the chain had at the beginning two vacancies between x_2 and x_3. After a first soliton like step the couple $(\mathrm{x}_1, \mathrm{x}_2)$ falls in the first vacancy but the second one is still there.

The finish of our treatment is an (x_2, x_3) section. Fig. 17 shows the 2D PES section for a fixed ion x_1 at 0.479 units, the value at the SP of Fig. 13. It is an SP of index one. The Min4 there now has disappeared. The NT (in brown color) to the direction $(0, 0, 1)$ for a push of ion x_3 is added for orientation. It is useless for the treatment of a soliton like behavior.

The aim of a movement of a soliton should be the translation of the full chain with x_3 at its new well at the place p6 at 3.6 units. It is the minimum Min5 in the upper region. However, neither an NT to a moderate movement

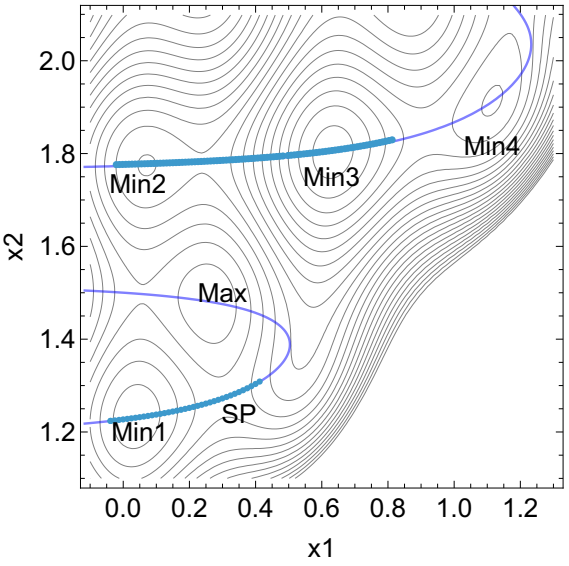

Fig. 16. 2D section of effective PES (1)/(3) for fixed x_3=3 and force $\mathbf{f}$=2.25 $(1,0,0)^T$ in Eq.(3), and also NT to direction $(1,0,0)$, compare Fig. 13. One can follow the movement of stationary points along the NT.

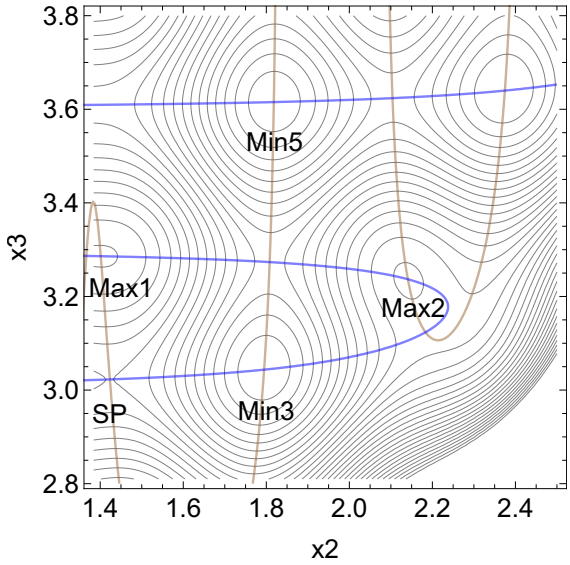

Fig. 17. 2D projected section of PES (1) for fixed x_1=0.479, the SP value of Fig. 14, brown is the NT to direction $(0,0,1)$, blue is the NT to direction $(0,1,0)$, see text.

in direction $(1,0,0)$ of only x_1, our initial beginning, nor the NT to collective direction $(1,1,0)$, or the push in direction of pure x_2 by $(0,1,0)$ gives a kind of soliton pattern like in Fig. 13. The direction to push the former couple of x_1, x_2 from Min 3 to Min5 is the pure third direction to x_3 represented by the brown NT. Before, there does not lead a usefull pathway from the SP in Fig. 17 to Min5, because in between is a valley-ridge inflection point [64,67,96], and any push to Min5 would need a push in x_3-direction. From Min3 to Min5 again a barrier has to be overcome. There is no direct way by a nearly flat mountain path form Min1 in Fig. 13 to Min5. It demonstrates that for two vacancies between the ions x_2 and x_3 no anti-kink soliton can exist. This would be a wave where an excitation of x_1 would be transported to x_3.

In a certain symmetry, starting in minimum Min3, one can see with Fig. 17 that a special excitation to pure x_2 by $\mathbf{f}^T$=$(0,1,0)$ could induce a partial soliton to the upper right minimum with x_2=2.4 and x_3=3.6 over the SP near the maximum. Again, this soliton like step surmounts only one vacancy. However, this structure would leave behind the x_1 at 0.6, and would also not be a translation of the initial chain.

Finally, we report that a very strong push of x_1 pushes together the chain like an harmonica, and can move this lump together along the substrate. However, this is also not the pattern of a soliton.

4.2 A further search for anti-kinks in a Wigner chain

The possibility of a soliton crucially depends on the configuration of the trap, the ratio of W_o and V_o in the potentials, and the proportion of the length a_s and d_o. A relation is given by the g-parameter [7]

$$g = \frac{k\, a_s^2}{8\, V_o} \,. \tag{4}$$

It is claimed that for $g \ll 1$ we expect pinning, but for $g \gg 1$ we expect the possibility of a sliding soliton. In former subsections, we have used $g = 0.21$ and obtain that a soliton is not possible. We found only a soliton like behavior of an ion pair. The too many vacuities destroy the possibility of solitons.

We try a next search for a larger g parameter with $V_o = 0.25$, the half value of the former studies. Fig. 18 shows three corresponding PES sections, in part A for $x_3 = 3$ fixed, in part B for $x_2 = 1.8$ fixed, but in part C for $x_1 = 0.6$ fixed. The different projections are to use for an illustration of the PES over the 3D coordinate space. We have to interpret the PES sections in the following kind: the former soliton like behavior of the pair (x_1, x_2) now again disappears. There is in part A no quasi-soliton-SP like in Fig. 13, but only a ridge of the PES remains with a TP of the NT to direction x_1. An excitation of ion x_1 from left into the chain is immediately redirected to a push on ion x_2 which moves to Min2, and only then x_1 moves to intermediate Min3. This Min3 is also shown in part B, and together with part C it is to see that from intMin3 only a move of the chain to Min5 is possible where x_3 has moved to a new global minimum. Min5 represents a full movement of the initial chain starting at Min1. Fig. 18 B additionally enrols a common pathway of the pair (x_1, x_3) like in Fig. 13 for the pair (x_1, x_2), the former quasi-soliton-pathway. Now the not nearest neighbors move combined, only the former quasi-soliton-SP is replaced by the quasi-soliton intMin3. The interaction of the first and the last ion is also obtained in the next subsection below. But at all, here it is not the behavior of a soliton of the full chain.

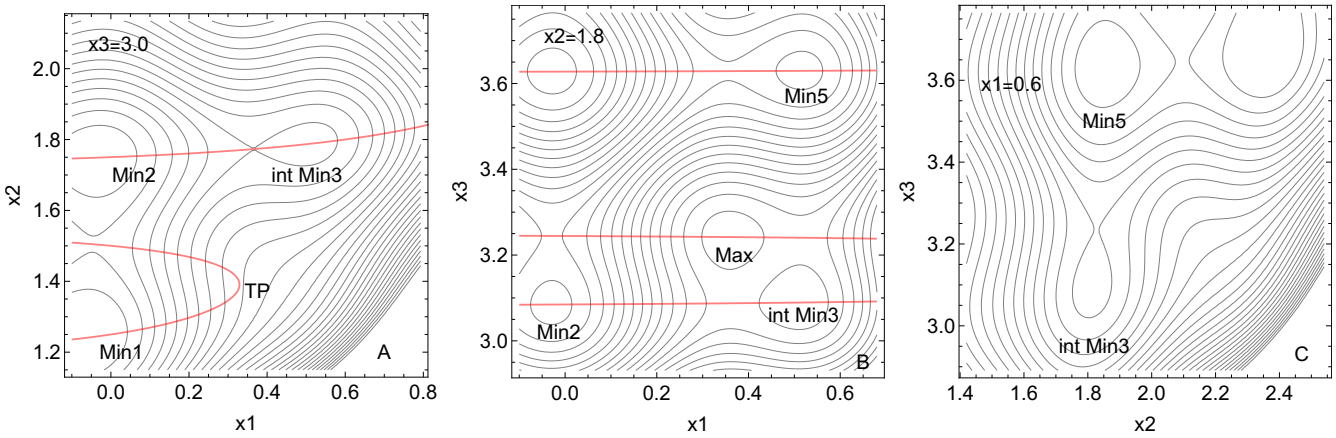

Fig. 18. 2D projected sections of PES (1) for changed parameter $V_o = 0.25$ and A) fixed x_3=3, B) fixed x_2=1.8, but C) fixed x_1=0.6. Note that the SP of Fig. 13 has disappeared in part A); only a TP of the NT remains. The red curve is the NT to direction $(1, 0, 0)$, correspondingly.

So, the assumption that an increase of the parameter g brings us nearer to a soliton is not fulfilled. We have to reject the importance of parameter g of Eq.(4).

4.3 The case of a vanishing trap

In contrast, if we further lower V_o, thus if we have $g \gg 1$ then we obtain more and more a pure Wigner chain with an unimportant substrate potential. Then the chain behaves like a Newton cradle [98]. If one pushes the left x_1 then this impulse flows through the chain transmitting a pressure wave through the stationary ions, which creates a force that pushes the last ion. Finally the right x_N ion flyes away. The remaining chain stays still on its former place. Again this is not the behavior of a soliton.

5 Discussion

We study in this paper a linear chain. Usually there is treated the possibility of a planar zig-zagging of the chain [48–52,55,58,59,97,99–109]. Then many kinds of distortions can become a soliton. This is excluded here.

Potential (2) is an approximation of potential (1) for local problems around a ground state structure of the chain. It can be used for vibrations or motional spectroscopy [43,110,111], for example. For a motion of parts of the chain by an antikink, or a kink, the problem is that a touching of the ions is not strong enough repelled in the potential (2). The Coulomb potential (1) has there singularities. This difference causes a somewhat different behavior against the soliton problem. The FK potential (2) with the given parameters [7] does not allow solitons. For the Wigner chain (1), in contrast, we find a partial soliton like behavior for couples of ions if only one vacancy is in between. However, for more than one vacancy between the ions, also here no antikink soliton is possible. Especially, a kink soliton is not probably from the definition of the potential (1). Since solitons are not expected in the chains discussed here, we will not find any type of conductance caused by moving ions, or by backward-moving vacancies [112].

For very longer chains, one should note that the central region of such a Wigner chain can be a little compressed [109] in comparison to the edge regions. The inter ionic spacing is a slowly varying function. However, this does not change our nutshell result here.

6 Conclusion

If there are many vacant sites of the laser field then we assume that a soliton will not find a 'flat' potential line like in many other cases of the FK model. In the figures emerge minima of different energy. They do not fit to the imagination for kinks or anti-kinks that the pinning energy in chains with reasonable parameters should be significantly lower than the amplitude of the substrate potential [74]. For a soliton one needs collective coordinates [113] for the center, $X(t)$, and the length, $l(t)$, of its structure. These cannot be defined here. In contrast, if the chain has overcome a barrier for a quasi soliton like movement, it immediately falls down into the next bowl with a corresponding energy step. A near zero force to move the soliton further cannot be found. Thus, for a chain with vacancies, a soliton behavior will become complicated, or should one say, impossible?

Declarations

Thanks to a reviewer for some important hints.
Funding
We acknowledge the financial support from the Spanish Structures of Excellence Mariá de Maeztu program, grant MDM-2017-0767 and Generalitat de Catalunya, project 2017 SGR 348.

Conflicts of interest
There is no conflict of competing interests.

Availability of data
Data of all stationary states reported in the paper are available on request by WQ.

Code
The Fortran code for the following of an NT, as well as the Mathematica codes for the calculation of stationary points of the WS, the NTs, and the representation of the Figures are available on request by WQ.

Authors' contributions
Both authors contributed equally to the manuscript.

References

1. E. Wigner, Phys. Rev. **46**, 1002 (1934)
2. H.J. Schulz, Phys. Rev. Lett. **71**, 1864 (1993)
3. I. Shapir, A. Hamo, S. Pecker, C.P. Moca, Ö. Legeza, G. Zarand, S. Ilani, Science **364**, 870 (2019)
4. C.C. Grimes, G. Adams, Phys. Rev. Lett. **42**, 795 (1979)
5. D.S. Fisher, B.I. Halperin, P.M. Platzman, Phys. Rev. Lett. **42**, 798 (1979)
6. H. Landa, C. Cormick, G. Morigi, Condensed Matter **5** (2020)
7. R. Menu, J.Y. Malo, V. Vuletic, M.L. Chiofalo, G. Morigi, Phys. Rev. B **110**, 224103 (2024)
8. K.A. Matveev, Phys. Rev. Lett. **92**, 106801 (2004)
9. K.A. Matveev, A. Furusaki, L.I. Glazman, Phys. Rev. B **76**, 155440 (2007)
10. K.A. Matveev, A.V. Andreev, M. Pustilnik, Phys. Rev. Lett. **105**, 046401 (2010)
11. G.A. Fiete, K.L. Hur, L. Balents, Phys. Rev. B **73**, 165104 (2006)
12. G.A. Fiete, Rev. Mod. Phys. **79**, 801 (2007)
13. A.E. Feiguin, G.A. Fiete, Phys. Rev. B **81**, 075108 (2010)
14. J.J. Wang, W. Li, S. Chen, G. Xianlong, M. Rontani, M. Polini, Phys. Rev. B **86**, 075110 (2012)
15. N. Traverso Ziani, F. Crépin, B. Trauzettel, Phys. Rev. Lett. **115**, 206402 (2015)
16. D. Vu, S.D. Sarma, Phys. Rev. B **101**, 125113 (2020)
17. X. Telleria-Allika, M.E. Azor, G. François, G.L. Bendazzoli, J.M. Matxain, X. Lopez, S. Evangelisti, J.A. Berger, J. Chem. Phys. **157**, 174107 (2022)
18. J.M. Luttinger, J. Math. Phys. **4**, 1154 (1963)
19. D.C. Mattis, E.H. Lieb, in *Bosonization*, edited by M. Stone (World Scientific Europe, 1965), Vol. 6, pp. 98–106
20. D.G. Rees, N.R. Beysengulov, J.J. Lin, K. Kono, Phys. Rev. Lett. **116**, 206801 (2016)
21. M.I. Dykman, Physics **9**, 54 (2016)
22. W. Quapp, J.Y. Lin, J.M. Bofill, Eur. Phys. J. B **93**, 227 (2020)
23. A.O. Badrutdinov, A.V. Smorodin, D.G. Rees, J.Y. Lin, D. Konstantinov, Phys. Rev. B **94**, 195311 (2016)
24. J.Y. Lin, A.V. Smorodin, A.O. Badrutdinov, D. Konstantinov, Phys. Rev. B **98**, 085412 (2018)
25. M. Pons, V. Ahufinger, C. Wunderlich, A. Sanpera, S. Braungardt, A. Sen(De), U. Sen, M. Lewenstein, Phys. Rev. Lett. **98**, 023003 (2007)
26. M. Johanning, A.F. Varon, C. Wunderlich, J. Phys. B: At. Mol. Opt. Phys. **42**, 154009 (2009)
27. C. Schneider, D. Porras, T. Schaetz, Rep. Progr. Phys. **75**, 024401 (2012)
28. C.D. Bruzewicz, J. Chiaverini, R. McConnell, J.M. Sage, Appl. Phys. Rev. **6**, 021314 (2019)
29. S. Mouradian, Physics **16**, 209 (2023)
30. J.S. Chen, E. Nielsen, M. Ebert, V. Inlek, K. Wright, V. Chaplin, A. Maksymov, E. Páez, A. Poudel, P. Maunz et al., Quantum **8**, 1516 (2024)
31. K. Sun, M. Kang, H.a. Nuomin, Nat. Commun. **16**, 4042 (2025)
32. V.V. Deshpande, M. Bockrath, Nature Phys. **4**, 314 (2008)
33. A. Secchi, M. Rontani, Phys. Rev. B **82**, 035417 (2010)
34. A. Secchi, M. Rontani, Phys. Rev. B **85**, 121410 (2012)
35. S. Pecker, F. Kuemmeth, A. Secchi, M. Rontani, D.C. Ralph, P.L. McEuen, S. Ilani, Nature Phys. **9**, 576 (2013)
36. N. Traverso Ziani, F. Cavaliere, M. Sassetti, Eur. Phys. Lett. **102**, 47006 (2013)
37. L. Sarkany, E. Szirmai, C.P. Moca, L. Glazman, G. Zarand, Phys. Rev. B **95**, 115433 (2017)
38. F.M. Gambetta, N. Traverso Ziani, F. Cavaliere, M. Sassetti, Eur. Phys. Lett. **107**, 47010 (2014)
39. Z. Xu, L. Li, G. Xianlong, S. Chen, J. Phys.: Condens. Matter **25**, 055601 (2013)
40. J. Hubbard, Phys. Rev. B **17**, 494 (1978)
41. D.H.E. Dubin, T.M. O'Neil, Rev. Mod. Phys. **71**, 87 (1999)
42. N. Traverso Ziani, F. Cavaliere, K. Guerrero Becerra, M. Sassetti, Crystals **11**, 20 (2021)
43. G. Morigi, S. Fishman, Phys. Rev. E **70**, 066141 (2004)
44. N. Defenu, G. Morigi, L. Dell'Anna, T. Enss, Phys. Rev. B **100**, 184306 (2019)
45. G. Birkl, S. Kassner, H. Walther, Nature **357**, 310 (1992)
46. M.G. Raizen, J.M. Gilligan, J.C. Bergquist, W.M. Itano, D.J. Wineland, Phys. Rev. A **45**, 6493 (1992)
47. D.H.E. Dubin, Phys. Rev. Lett. **71**, 2753 (1993)
48. S. Fishman, G. De Chiara, T. Calarco, G. Morigi, Phys. Rev. B **77**, 064111 (2008)
49. S. Ulm, J. Roßnagel, G. Jacob, C. Degünther, S.T. Dawkins, U.G. Poschinger, R. Nigmatullin, A. Retzker, M.B. Plenio, F. Schmidt-Kaler et al., Nat Commun **4**, 2290 (2013)
50. K. Pyka, J. Keller, H. Partner, R. Nigmatullin, T. Burgermeister, D. Meier, K. Kuhlmann, A. Retzker, M. Plenio, W. Zurek et al., Nature Commun. **4**, 2291 (2013)
51. M. Mielenz, J. Brox, S. Kahra, G. Leschhorn, M. Albert, T. Schaetz, H. Landa, B. Reznik, Phys. Rev. Lett. **110**, 133004 (2013)
52. S. Ejtemaee, P.C. Haljan, Phys. Rev. A **87**, 051401 (2013)
53. J. Brox, P. Kiefer, M. Bujak, T. Schaetz, H. Landa, Phys. Rev. Lett. **119**, 153602 (2017)
54. J. Kiethe, R. Nigmatullin, D. Kalincev, T. Schmirander, T. Mehlstäubler, Nature Commun. **8**, 15364 (2017)
55. J. Kiethe, R. Nigmatullin, T. Schmirander, D. Kalincev, T.E. Mehlstäubler, New J. Phys. **20**, 123017 (2018)
56. D.A. Gangloff, A. Bylinskii, V. Vuletić, Phys. Rev. Research **2**, 013380 (2020)
57. J. Eschner, G. Morigi, F. Schmidt-Kaler, R. Blatt, J. Opt. Soc. Am. B **20**, 1003 (2003)
58. E. Shimshoni, G. Morigi, S. Fishman, Phys. Rev. Lett. **106**, 010401 (2011)

59. J. Zhang, B.T. Chow, S. Ejtemaee, P.C. Haljan, npj Quant. Inform. **9**, 68 (2023)
60. P.M. Bonetti, A. Rucci, M.L. Chiofalo, V. Vuletić, Phys. Rev. Res. **3**, 013031 (2021)
61. L. Timm, L.A. Rüffert, H. Weimer, L. Santos, T.E. Mehlstäubler, Phys. Rev. Res. **3**, 043141 (2021)
62. A. Vanossi, N. Manini, M. Urbakh, S. Zapperi, E. Tosatti, Rev. Mod. Phys. **85**, 529 (2013)
63. T. Zanca, F. Pellegrini, G.E. Santoro, E. Tosatti, Proc. Nat. Acad. Sci. **115**, 3547 (2018)
64. W. Quapp, J.M. Bofill, Molec. Phys. **117**, 1541 (2019)
65. D.G. Rees, S.S. Yeh, B.C. Lee, K. Kono, J.J. Lin, Phys. Rev. B **96**, 205438 (2017)
66. J.Y. Lin, A.V. Smorodin, A.O. Badrutdinov, D. Konstantinov, J. Low Temp. Phys. **195**, 289 (2019)
67. W. Quapp, J.M. Bofill, Theoret. Chem. Acc. **135**, 113 (2016)
68. W. Quapp, J.M. Bofill, J. Ribas-Ariño, Int. J. Quant. Chem. **118**, e25775 (2018)
69. J.M. Bofill, J. Ribas-Ariño, S.P. García, W. Quapp, J. Chem. Phys. **147**, 152710 (2017)
70. W. Quapp, J.M. Bofill, Int. J. Quant. Chem. **118**, e25522 (2018)
71. P. Mezey, *Potential Energy Hypersurfaces* (Elsevier, Amsterdam, 1987)
72. D. Heidrich, W. Kliesch, W. Quapp, *Properties of Chemically Interesting Potential Energy Surfaces* (Springer, Berlin, Heidelberg, 1991)
73. B. Joos, Solid State Comm. **42**, 709 (1982)
74. I.A. Abronin, N.M. Kuznetsova, I.D. Mikheikin, V.P. Sakun, Russ. J. Phys. Chem. B **10**, 203 (2016)
75. W. Quapp, J.M. Bofill, Molec. Phys. **117**, 1541 (2019)
76. B.A. Malomed, Low Temp. Phys. **48**, 856 (2022)
77. N.J. Zabusky, M.D. Kruskal, Phys. Rev. Lett. **15**, 240 (1965)
78. O. Braun, Y. Kivshar, *The Frenkel-Kontorova Model: Concepts, Methods, and Applications* (Springer, New York, 2004)
79. W. Quapp, J.M. Bofill, European Phys. J. B **92**, 193 (2019)
80. W. Quapp, J.M. Bofill, European Phys. J. B **92**, 95 (2019)
81. W. Quapp, J.M. Bofill, European Phys. J. B **94**, 66 (2021)
82. W. Quapp, J.M. Bofill, European Phys. J. B **94**, 64 (2021)
83. W. Quapp, J.M. Bofill, J. Statist. Mech. **2022**, 013204 (2022)
84. W. Quapp, J.M. Bofill, European Phys. J. B **95**, 87 (2022)
85. W. Quapp, J.M. Bofill, arXiv2210.070000 (2022)
86. W. Quapp, J.M. Bofill, Leibniz Online **49**, 1 (2023)
87. C. Cormick, G. Morigi, Phys. Rev. A **87**, 013829 (2013)
88. S. Stoyanov, H.Müller-Krumhaar, Surf. Sci. **159**, 49 (1985)
89. M.E. Azor, L. Brooke, S. Evangelisti, T. Leininger, P.F. Loos, N. Suaud, J.A. Berger, SciPost Phys. Core **1**, 001 (2019)
90. M. Romero-Bastida, A.G. Martínez-Rosas, J. Stat. Mech. **2022**, 123205 (2022)
91. N. Beraha, A. Soba, M.F. Carusela, J. Phys. A **55**, 1 (2022)
92. O. Chelpanova, S.P. Kelly, G. Morigi, F. Schmidt-Kaler, J. Marino, Europhys. Lett. **143**, 25002 (2023)
93. T. Lauprêtre, R.B. Linnet, I.D. Leroux, H. Landa, A. Dantan, M. Drewsen, Phys. Rev. A **99**, 031401 (2019)
94. M. Weegen, M. Poggio, S. Willitsch, Phys. Rev. Lett. **133**, 223201 (2024)
95. H.K. Li, E. Urban, C. Noel, A. Chuang, Y. Xia, A. Ransford, B. Hemmerling, Y. Wang, T. Li, H. Häffner et al., Phys. Rev. Lett. **118**, 053001 (2017)
96. W. Quapp, M. Hirsch, O. Imig, D. Heidrich, J. Comput. Chem. **19**, 1087 (1998)
97. H. Landa, B. Reznik, J. Brox, M. Mielenz, T. Schaetz, New J. Phys. **15**, 093003 (2013)
98. F. Herrmann, M. Seitz, Amer. J. Phys. **50**, 977 (1982)
99. J.M.P. Carmelo, P.D. Sacramento, T. Stauber, D.K. Campbell, Phys. Rev. Research **5**, 043058 (2023)
100. Isha, A.K. Bera, G. Kaur, C. Stock, K. Chakraborty, P. Puphal, M. Isobe, K. Küster, Y. Skourski, L. Bhaskaran et al., Phys. Rev. Research **6**, L032010 (2024)
101. G. Piacente, I.V. Schweigert, J.J. Betouras, F.M. Peeters, Phys. Rev. B **69**, 045324 (2004)
102. G. Piacente1, G.Q. Hai1, F.M. Peeters, Phys. Rev. B **81**, 024108 (2010)
103. J. Kiethe, L. Timm, H. Landa, D. Kalincev, G. Morigi, T.E. Mehlstäubler, Phys. Rev. B **103**, 104106 (2021)
104. P. Silvi, G. De Chiara, T. Calarco, G. Morigi, S. Montangero, Annal. Phys. **525**, 827 (2013)
105. S. Ganguly, K. Mondal, S.K. Maiti, J. Appl. Phys. **136**, 104301 (2024)
106. J. Wang, K. Kong, X. Ma, J. Guan, X. Liu, C. Jin, H. Pan, Z. Liu, R. Tang, Chem **10**, 843 (2024)
107. J. Gao, H. Cao, X. Hu, H. Zhou, Z. Cai, Q. Zhao, D. Li, Z. Gao, S. Ideta, K. Shimada et al., Phys. Rev. Lett. **134**, 086202 (2025)
108. P.L. Christiansen, A.V. Savin, A.V. Zolotaryuk, Phys. Rev. B **54**, 12892 (1996)
109. A. del Campo, G. De Chiara, G. Morigi, M.B. Plenio, A. Retzker, Phys. Rev. Lett. **105**, 075701 (2010)
110. M. Cetina, A. Bylinskii, L. Karpa, D. Gangloff, K.M. Beck, Y. Ge, M. Scholz, A.T. Grier, I. Chuang, V. Vuletić, New J. Phys. **15**, 053001 (2013)
111. L. Timm, H. Weimer, L. Santos, T.E. Mehlstäubler, Phys. Rev. B **108**, 134302 (2023)
112. H.U. Beyeler, L. Pietronero, S. Strässler, Phys. Rev. B **22**, 2988 (1980)
113. M. Salerno, Y. Zolotaryuk, Phys. Rev. E **65**, 056603 (2002)